Immunity
Article

The Essential Functions of Adipo-osteogenic Progenitors as the Hematopoietic Stem and Progenitor Cell Niche

Yoshiki Omatsu,[1] Tatsuki Sugiyama,[1] Hiroshi Kohara,[1] Gen Kondoh,[2] Nobutaka Fujii,[3] Kenji Kohno,[4] and Takashi Nagasawa[1,*]
[1]Department of Immunobiology and Hematology
[2]Laboratory of Animal Experiments for Regeneration, Institute for Frontier Medical Sciences
Kyoto University, 53 Kawahara-cho, Shogoin, Sakyo-ku, Kyoto 606-8507, Japan
[3]Graduate School of Pharmaceutical Sciences, Kyoto University, Sakyo-ku, Kyoto 606-8501, Japan
[4]Laboratory of Molecular and Cell Genetics, Graduate School of Biological Sciences, Nara Institute of Science and Technology (NAIST), 8916-5 Takayama, Ikoma, Nara 630-0192, Japan
*Correspondence: tnagasa@frontier.kyoto-u.ac.jp
DOI 10.1016/j.immuni.2010.08.017

SUMMARY

Hematopoietic stem cells (HSCs) and their lympho-hematopoietic progeny are supported by microenvironmental niches within bone marrow; however, the identity, nature, and function of these niches remain unclear. Short-term ablation of CXC chemokine ligand (CXCL)12-abundant reticular (CAR) cells in vivo did not affect the candidate niches, bone-lining osteoblasts, or endothelial cells but severely impaired the adipogenic and osteogenic differentiation potential of marrow cells and production of the cytokines SCF and CXCL12 and led to a marked reduction in cycling lymphoid and erythroid progenitors. HSCs from CAR cell-depleted mice were reduced in number and cell size, were more quiescent, and had increased expression of early myeloid selector genes, similar to the phenotype of wild-type HSCs cultured without a niche. Thus, the niche composed of adipo-osteogenic progenitors is required for proliferation of HSCs and lymphoid and erythroid progenitors, as well as maintenance of HSCs in an undifferentiated state.

INTRODUCTION

Hematopoietic stem cells (HSCs) give rise to all lineages of blood cells, including immune cells in the bone marrow. It has been assumed that the special microenvironments known as niches play an essential role in maintaining HSCs and hematopoietic progenitors in the marrow to provide appropriate numbers of mature blood cells throughout life (Morrison and Spradling, 2008; Wilson and Trumpp, 2006). HSCs and lymphoid progenitors are thought to reside in their niches, and the identity of the niche has been a subject of longstanding debate. It has been shown that HSCs are in contact with a population of osteoblasts lining the bone surface, termed spindle-shaped N-cadherin^{+}CD45^{-} osteoblastic (SNO) cells, which express a high amount of N-cadherin (endosteal niches) (Zhang et al., 2003). In contrast, many HSCs are associated with sinusoidal endothelium, suggesting that endothelial cells create cellular niches for HSCs (vascular niches) (Kiel et al., 2005). We have shown that CXCR4, a primary receptor for the CXC chemokine ligand (CXCL)12 (also known as stromal cell-derived factor-1) (Nagasawa, 2006; Nagasawa et al., 1996; Nagasawa et al., 1994; Tachibana et al., 1998; Zou et al., 1998), is essential for maintaining a pool of HSCs and B cells and that most HSCs, early B cell precursors, and plasma cells are scattered throughout the bone marrow cavity and are in contact with a small population of reticular cells with long processes, expressing high amounts of CXCL12, called CXCL12-abundant reticular (CAR) cells, suggesting that CAR cells are a key component of niches for both HSCs and B cells (Nagasawa, 2008; Sugiyama et al., 2006; Tokoyoda et al., 2004). However, these studies do not reveal the functions of SNO cells, endothelial cells, and CAR cells as niches for HSCs and/or lymphoid progenitors.

Prior studies using a variety of gain-of-function and loss-of-function approaches examined the identity and functions of cellular niches for HSCs and hematopoietic progenitors. Bone morphogenetic protein (BMP) receptor type IA (BMPRIA) conditionally deficient mice displayed increases in the numbers of SNO cells, which correlated with an increase in the numbers of HSCs (Zhang et al., 2003). Parathyroid hormone (PTH) administration increased the numbers of osteoblasts in culture and induced an increase in the number of HSCs in vivo (Calvi et al., 2003). In contrast, it has been shown that depleting osteoblastic lineage cells with a 2.3 kb fragment from the rat type I collagen α1 (Col1α1) gene promoter driving thymidine kinase (Col2.3ΔTK) induced a marked reduction in hematopoietic cells (Visnjic et al., 2004; Zhu et al., 2007). These results suggest that osteoblastic lineage cells maintain HSCs and hematopoietic cells but do not rule out the possibility that Col1α1, BMPRIA, and PTH or PTH-related protein receptor (PPR) are expressed in bone marrow reticular cells, including CAR cells. In addition, it has been reported that reductions in osteoblasts do not necessarily lead to reductions in HSCs and hematopoietic cells (Kiel et al., 2007; Wilson and Trumpp, 2006). Together, it remains unresolved which cell types play major roles in regulating the

maintenance of HSCs and lymphoid progenitors within bone marrow.

It is assumed that most adult HSCs are quiescent and that HSC quiescence is maintained by their niches (Arai et al., 2004; Orford and Scadden, 2008). In contrast, many studies have shown that the majority of HSCs are cycling, albeit slowly, although some HSCs are highly dormant, (Cheshier et al., 1999; Foudi et al., 2009; Santaguida et al., 2009; Wilson et al., 2008; Yamazaki et al., 2006) and that many lineage-restricted progenitors are known to be cycling actively, supporting the idea that HSC and hematopoietic progenitor proliferation is maintained by their niches. However, the technology to prove this was lacking and the role of niches in controlling the quiescence, proliferation, and differentiation of HSCs and lymphoid progenitors remain unclear. Here, we generated mice that allow selective ablation of CAR cells in bone marrow and determined the nature and in vivo function of CAR cells as a niche for HSCs and lympho-hematopoietic progenitors.

RESULTS

Generation of Mice that Allow Inducible Selective Ablation of CAR Cells In Vivo

To determine the nature and in vivo function of CAR cells, we generated mice in which a transgene encoding the Diphtheria toxin (DT) receptor-green fluorescent protein (DTR-GFP) fusion protein (Saito et al., 2001) was knocked into the *Cxcl12* locus (CXCL12-DTR-GFP mice) (Figure 1A). These mice allow the conditional ablation of CXCL12-expressing cells by DT administration because wild-type murine cells are insensitive to killing by DT (Saito et al., 2001). CXCL12-DTR-GFP mice were injected intraperitoneally (i.p.) with DT at a dose of 25 ng/kg; many mice remained healthy for up to 3 days after injection and died 5 days after injection probably from liver failure. By histological analysis, the liver of CXCL12-DTR-GFP mice showed necrosis and haemorrhage at 5 days after DT treatment but appeared normal at 2 days after DT treatment. Histological analysis of bone marrow microenvironments 2 or 3 days after DT treatment revealed that CXCL12-DTR-GFP^{+} CAR cells were eliminated or severely reduced, but bone-lining SNO cells, osteocalcin^{+} or marked alkaline phosphatase (ALP) activity-containing osteoblasts, and sinusoidal endothelial cells remained unaffected in DT-treated CXCL12-DTR-GFP mice compared with untreated CXCL12-DTR-GFP mice (Figures 1B and 1C; Figure S1 available online; data not shown). Flow-cytometric analysis confirmed that the numbers of CXCL12-DTR-GFP^{hi} CAR cells were severely reduced in DT-treated CXCL12-DTR-GFP mice compared with untreated animals (Figure 1E). In addition, consistent with the result that CAR cells are a small population of VCAM-1^{+} reticular cells (Tokoyoda et al., 2004), many VCAM-1^{+} reticular cells were observed in DT-treated and untreated CXCL12-DTR-GFP mice (Figure 1D).

Short-Term Ablation of CAR Cells Leads to a Reduction in Cycling Lymphoid and Erythroid Progenitors

To better define the direct effect of CAR cell depletion on hematopoiesis, we examined the effect of short-term ablation of CAR cells on hematopoietic cells in the bone marrow using CXCL12-DTR-GFP mice 2 days after DT treatment, in which CAR cells were eliminated or severely reduced. Total bone marrow cellularity was reduced in DT-treated CXCL12-DTR-GFP mice compared with DT-treated and untreated wild-type mice (Figure 2A and Figure S2A). Flow-cytometric analysis of hematopoietic progenitors revealed that although the numbers of Lineage(Lin)$^{-}$Sca-1^{+}c-kit^{+}Flt3^{+} multipotent progenitors (MPPs) (Adolfsson et al., 2001) appeared normal, Lin^{-}IL-7Rα^{+}Flt3^{+} common lymphoid progenitors (CLPs) (Karsunky et al., 2008) and c-kit^{+}CD71^{+}Ter119^{lo} proerythroblasts were almost absent, the numbers of c-kit^{+}CD19^{+}IgM^{-} pro-B cells and Lin^{-}Sca-1^{-}c-kit^{+}CD34^{-}FcγRII-III^{lo} megakaryocyte and erythrocyte progenitors (MEPs) (Akashi et al., 2000) were severely reduced and the number of Lin^{-}Sca-1^{-}c-kit^{+}CD34^{+}FcγRII-III^{hi} granulocyte and macrophage progenitors (GMPs) (Akashi et al., 2000) was more modestly reduced in DT-treated CXCL12-DTR-GFP mice compared with untreated CXCL12-DTR-GFP mice or DT-treated and untreated wild-type mice (Figures 2B and 2C and Figure S2A). Cell-cycle analysis of pro-B cells and MEPs using Pyronin Y (PY) revealed that around half of the cells were cycling actively (high PY fluorescence [PY^{hi}]) and other quiescent cells displayed low PY fluorescence (PY^{lo}) in DT-treated wild-type mice. In contrast, a reduction in the frequency of PY^{hi} cells and an increase in the frequency of PY^{lo} cells were observed in DT-treated CXCL12-DTR-GFP mice (Figure 2D). Additionally, Annexin-V staining of pro-B cells revealed many apoptotic cells (43%) in DT-treated CXCL12-DTR-GFP mice although few (5.1%) were detected in DT-treated wild-type mice (Figure 2E). These results indicate that CAR cells are essential for lymphoid, erythroid, and myeloid lineage development and suggest that CAR cells support the survival and proliferation of B cell progenitors and proliferation of erythroid progenitors.

HSCs Are Reduced and More Quiescent in the Absence of CAR Cells

We next examined the effect of short-term ablation of CAR cells on HSCs. Bone marrow from CXCL12-DTR-GFP and wild-type mice was analyzed 2 days after DT treatment. The number of CD34^{-}Lin^{-}Sca-1^{+}c-kit^{+}CD150^{+}CD48^{-} cells, which are highly enriched for long-term repopulating HSCs (Foudi et al., 2009; Kiel et al., 2005; Wilson et al., 2008), was reduced, but to a lesser extent than lymphoid and erythroid progenitors in DT-treated CXCL12-DTR-GFP mice compared with control animals (Figure 3A and Figure S3A). Because the unambiguous measure of HSCs is long-term transplantation, we estimated the numbers of HSCs using repopulating units (RU), based on a competitive repopulation assay (Harrison et al., 1993). The numbers of RU were reduced about 50% in the bone marrow of CXCL12-DTR-GFP mice compared with wild-type mice (Figure 3B), indicating that CAR cells play an essential role in maintaining the HSC number.

Flow-cytometric analysis using the proliferation marker Ki67 has shown that a small percentage of CD34^{-}Lin^{-}Sca-1^{+}c-kit^{+}CD48^{-} HSCs express Ki67 in DT-treated or untreated wild-type mice, as reported previously, but the numbers of Ki67-positive cells were severely reduced in the HSC population from DT-treated CXCL12-DTR-GFP mice (Figure 3C). Quantitative, real-time polymerase chain reaction with reverse transcription (qRT-PCR) analysis revealed that the mRNA expression of Evi-1 and Pbx1, which are essential for HSC maintenance and

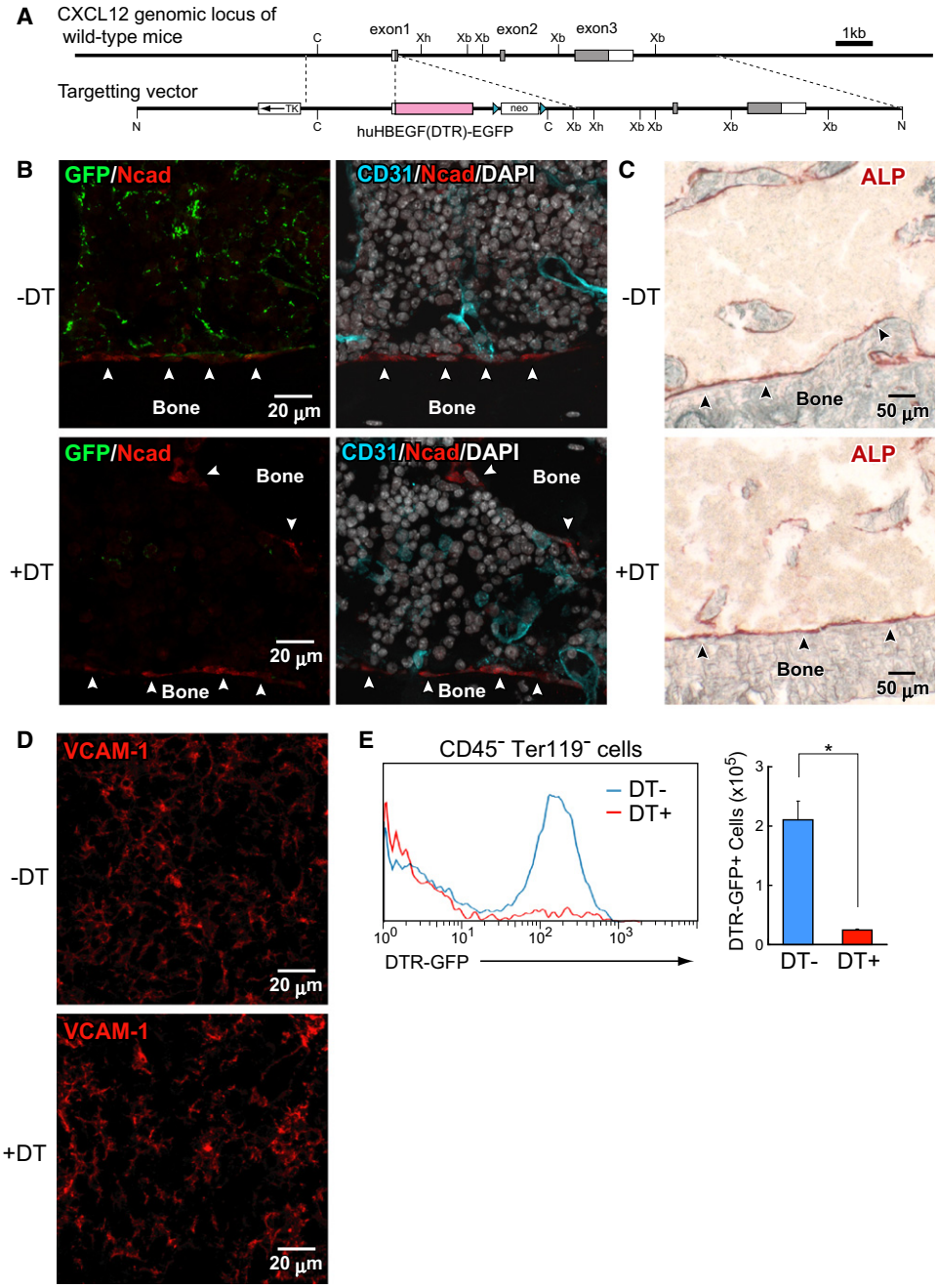

Figure 1. Short-Term Selective Ablation of CAR Cells In Vivo in Bone Marrow

(A) Strategy used to generate CXCL12-DTR-GFP mice. C, Csp45I; Xh, XhoI; Xb, XbaI; N, NotI. Triangles represent LoxP sites.

(B–E) Bone marrow from CXCL12-DTR-GFP mice was analyzed 2 days after administration of DT or control vehicle. Bone marrow sections were stained with antibodies against GFP, N-cadherin, the panendothelial marker PECAM-1 (CD31) (B), and VCAM-1 (D) and assayed by Fast Red staining (C). CXCL12-DTR-GFP^{+} CAR cells (green) are eliminated (B, left); however, bone-lining SNO cells detected by anti-N-cadherin antibodies (B, arrowheads; red), marked ALP activity-containing osteoblasts (C, arrowheads; red), and sinusoidal endothelial cells (B, right; blue) exhibit normal numbers and morphology in DT-treated CXCL12-DTR-GFP mice. The nuclei of cells were labeled with DAPI dye (B, right; white). (E) Flow cytometric analysis of CD45^{-}Ter119^{-}CD31^{-} nonhematopoietic cells. The numbers of CXCL12-DTR-GFP^{hi} CAR cells per two femurs and tibiae are shown (E, right). All error bars represent SD of the mean. n = 4; *p < 0.05.

preferentially expressed in HSCs (Ficara et al., 2008; Goyama et al., 2008), was largely unaffected in the HSC population from DT-treated CXCL12-DTR-GFP mice (Figure 3D and Figure S3C). In contrast, although cell-cycle-promoting genes, including those that encode Cyclin D1, D2, A2, and their catalytic partner, Cdc2a, and a regulator of initiation of DNA replication, Cdc6, were expressed in the HSC population from DT-treated and untreated wild-type mice and untreated CXCL12-DTR-GFP

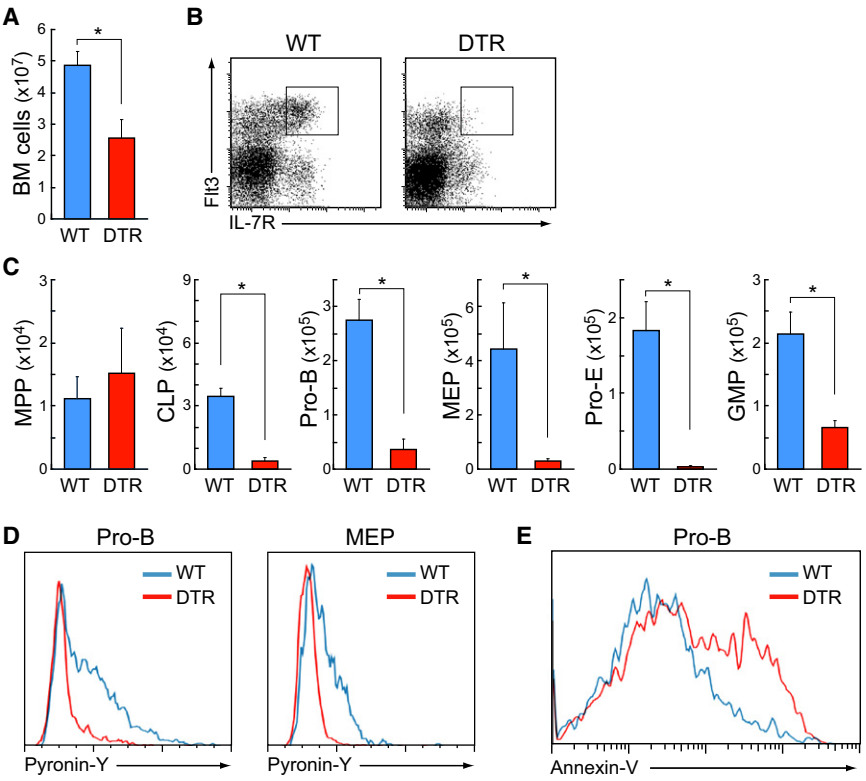

Figure 2. Essential In Vivo Functional Roles of CAR Cells in Lympho-hematopoietic Progenitors

Bone marrow from wild-type and CXCL12-DTR-GFP mice was analyzed by flow cytometry 2 days after DT administration.

(A) Total numbers of $CD45^+$ hematopoietic cells per two femurs and tibiae. n = 3; *p < 0.05.

(B) Immunofluorescent profiles of CLPs. Gated Lin^- cells are analyzed for the expression of IL-7Rα and Flt3.

(C) The numbers of MPPs, CLPs, pro-B cells, MEPs, proerythroblasts (pro-E), and GMPs per two femurs and tibiae. n = 3; *p < 0.05.

(D) RNA content of pro-B cells and MEPs by PY staining.

(E) Annexin-V staining of pro-B cells.

All error bars represent SD of the mean (A and C).

mice, consistent with previous studies (Kalaszczynska et al., 2009; Kozar et al., 2004; Santaguida et al., 2009; Yamazaki et al., 2006), expression of these genes was markedly reduced in the HSC population from DT-treated CXCL12-DTR-GFP mice (Figure 3D and data not shown). In addition, mRNA expression of the transcriptional repressor Mad1, considered to decrease cell size (Iritani et al., 2002) and inhibit HSC proliferation (Walkley et al., 2005), was significantly elevated in the HSC population from DT-treated CXCL12-DTR-GFP mice (Figure 3D). Cellular activation by growth factors induces entry into a phase of cell cycle characterized by initiation of transcription and accumulation of RNA, mainly in the form of ribosomal RNA, which can be measured by RNA-specific dyes, such as PY. As reported previously, almost all $CD34^-Lin^-Sca\text{-}1^+c\text{-}kit^+CD48^-$ HSCs from DT-treated wild-type mice displayed low PY fluorescence (Figure 3E); however, PY fluorescence in many HSCs from DT-treated CXCL12-DTR-GFP mice decreased further compared with wild-type mice (Figure 3E). Furthermore, in DT-treated CXCL12-DTR-GFP mice, most cells in the HSC population were smaller than those in control animals, shown by forward scatter characteristics (FSCs) on flow cytometry, although Annexin-V staining revealed no increase in apoptotic cells in the population (Figure 3F and Figure S3D). Histological analysis of the bone marrow from DT-treated CXCL12-DTR-GFP mice, in which CAR cells were severely reduced, revealed that $CD150^+CD48^-CD41^-$ HSCs, which did not adjoin CAR cells, were significantly smaller than HSCs in contact with the processes of residual CAR cells, indicating that short-term ablation of CAR cells leads to a significant decrease in the cell size of adjacent HSCs (Figures 3G and 3H).

Together, these results indicate that HSCs are more quiescent in CAR cell-depleted mice and that CAR cells keep HSCs in a proliferative state.

Short-Term Ablation of CAR Cells Induces Early Myeloid Differentiation of HSCs

It is unclear whether HSC niches regulate the differentiation of HSCs. To address this issue, we analyzed the expression of genes that encode activities important for HSC differentiation in the HSC population from CAR cell-depleted mice. It has been shown that elevating the expression of transcription factor PU.1 in primitive multipotent progenitors induces the generation of myeloid lineage (Arinobu et al., 2007; DeKoter and Singh, 2000). Of note, qRT-PCR analysis revealed that the mRNA expression of PU.1 and its macrophage-specific target M-CSF receptor (M-CSFR) was markedly increased in the $CD34^-Lin^-Sca\text{-}1^+c\text{-}kit^+CD150^+CD48^-$ HSC population from CXCL12-DTR-GFP mice 2 days after DT treatment, compared with untreated CXCL12-DTR-GFP mice or DT-treated and untreated wild-type mice (Figure 3I and data not shown).

Cells in the HSC population were sorted from bone marrow of wild-type and CXCL12-DTR-GFP mice 2 days after DT treatment and cultured in the presence of SCF and CXCL12, which support myeloid differentiation from HSCs and more mature multipotent progenitors. Flow-cytometric analysis showed that substantial numbers of $Gr\text{-}1^{hi}CD11b^+$ myeloid lineage cells were generated from wild-type HSCs at day 10 of culture and peaked at day 14 or later (data not shown). In contrast, cells in the HSC population from CAR cell-depleted mice had generated substantial numbers of $Gr\text{-}1^{hi}CD11b^+$ myeloid lineage cells earlier, day 7 of culture, and peaked at day 10, supporting the idea that some cells in the HSC population from CAR cell-depleted mice are more differentiated than in wild-type mice (Figure 3J and data not shown). Together, these results suggest that short-term CAR cell depletion prevented HSC maintenance in an undifferentiated state.

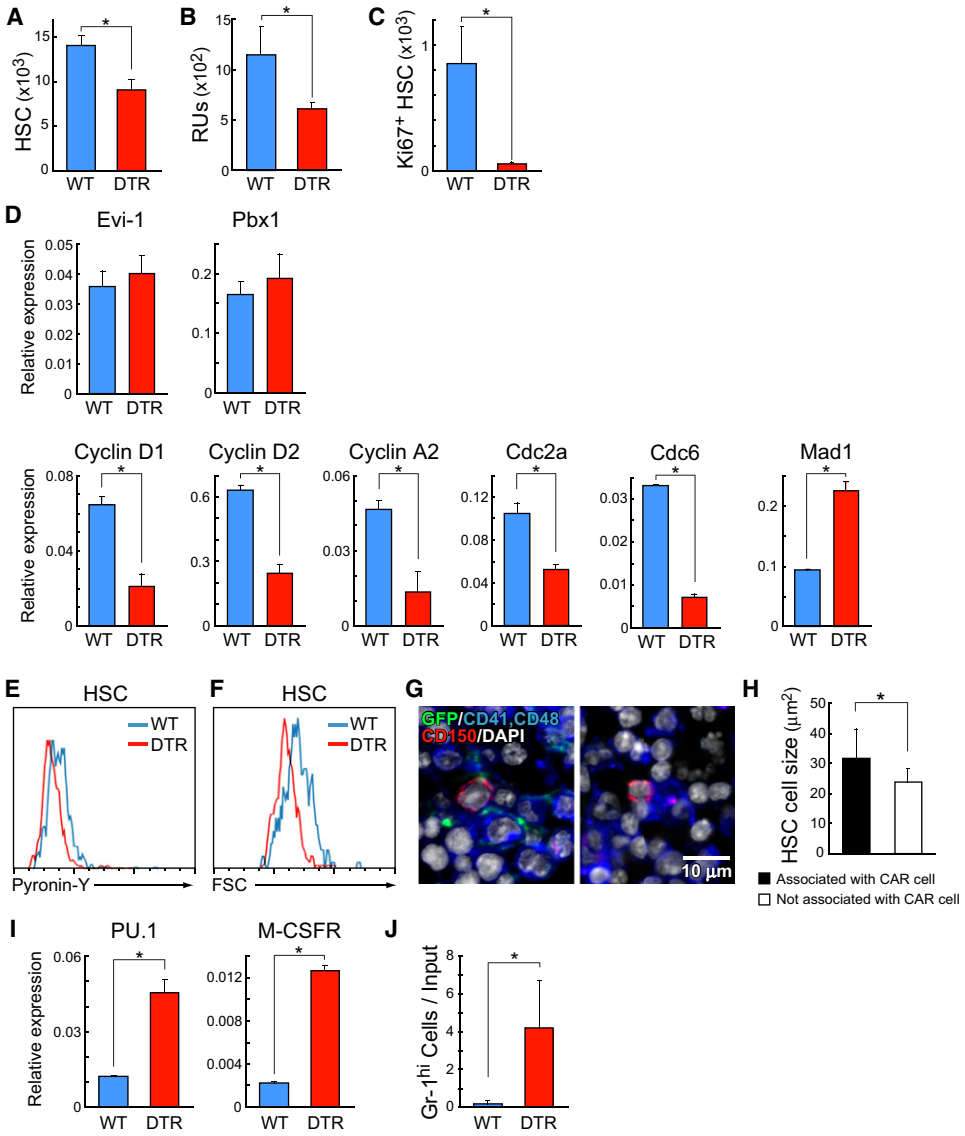

Figure 3. Essential In Vivo Functional Roles of CAR Cells in HSCs

Bone marrow from wild-type and CXCL12-DTR-GFP mice was analyzed 2 days after DT administration.

(A) Flow-cytometric analysis of the numbers of cells in the CD34$^-$Lin$^-$Sca-1$^+$c-kit$^+$CD150$^+$CD48$^-$ HSC population per two femurs and tibiae. n = 3; *p < 0.05.

(B) The numbers of HSCs were estimated using repopulating units (RU), based on a competitive repopulation assay. n = 3; *p < 0.05.

(C) Flow-cytometric analysis of the numbers of Ki67-positive cells in the HSC population per two femurs and tibiae. n = 3; *p < 0.05.

(D) Relative mRNA expression levels of Evi-1, Pbx1, Cyclin D1, D2, A2, Cdc2a, Cdc6, and Mad1 in sorted cells in the HSC population by qRT-PCR analysis normalized to G3PDH levels. n = 4; *p < 0.05.

(E) Flow-cytometric analysis of RNA content of cells in the HSC population by PY staining.

(F) Flow-cytometric analysis of cell size of cells in the HSC population by FSC.

(G and H) Sections of bone marrow from DT-treated CXCL12-DTR-GFP mice were stained with antibodies against CD150, CD48, and CD41. Cell size of CD150$^+$CD48$^-$CD41$^-$ HSCs in contact with (G, left) or at a distance from remaining CAR cells (G, right) was determined using a confocal microscope and its software (H). n = 20; *p < 0.05.

(I) Relative mRNA expression levels of PU.1 and M-CSFR in sorted cells in the HSC population by qRT-PCR analysis normalized to G3PDH levels. n = 4; *p < 0.05.

(J) Generation of myeloid lineage cells from cells in the HSC population in culture at an early point of time. Sorted cells in the HSC population were cultured in the presence of SCF and CXCL12. Flow-cytometric analysis of the numbers of Gr-1^{hi}CD11b$^+$ cells per input cell at day 7 of culture. n = 4; *p < 0.05. All error bars represent SD of the mean (A–D and H–J).

DT Does Not Act Directly on Hematopoietic Cells in CXCL12-DTR-GFP Mice

To rule out the possibility that DT acted directly on hematopoietic cells in DT-treated CXCL12-DTR-GFP mice, we infused bone marrow cells from CXCL12-DTR-GFP or wild-type mice into lethally irradiated recipients in the absence of competitor cells. When bone marrow hematopoietic cells of chimeric mice were mainly derived from donor HSCs 12 weeks after transplantation,

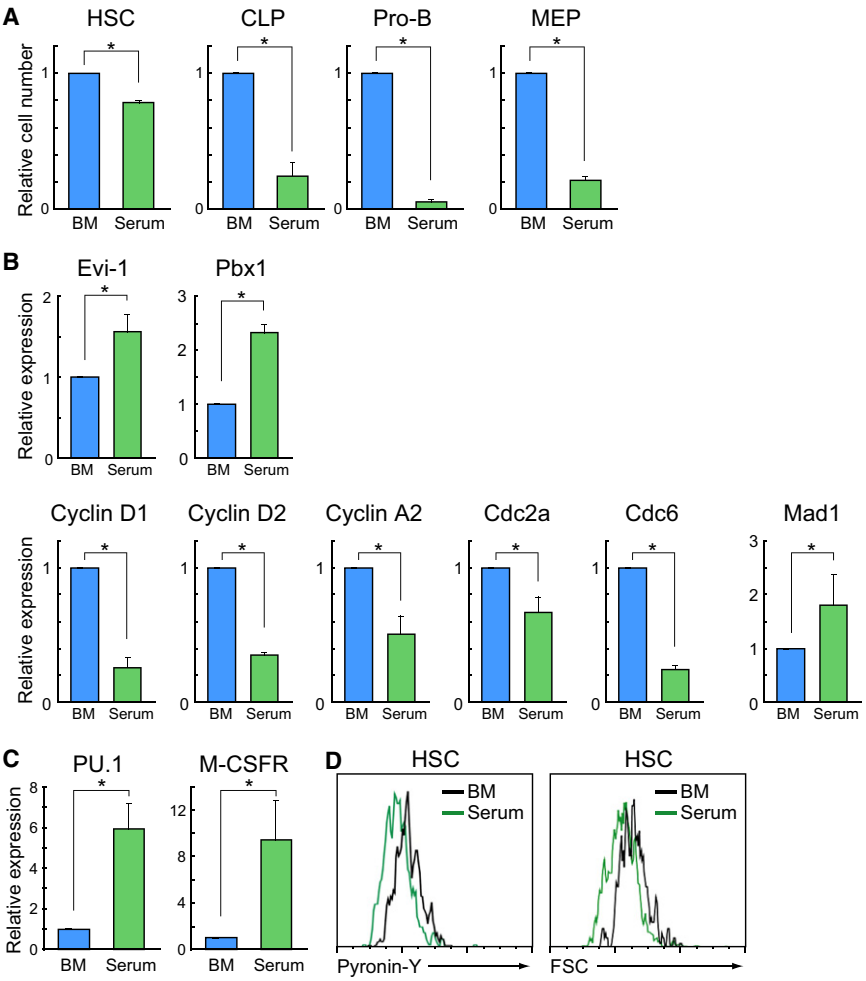

Figure 4. The Phenotypes of Wild-Type HSCs and Lympho-hematopoietic Progenitors Cultured in Serum Alone

(A) Single CD34$^-$Lin$^-$Sca-1$^+$c-kit$^+$CD150$^+$CD48$^-$ HSCs, CLPs, pro-B cells, and MEPs from wild-type mice were sorted and cultured in serum alone (1 cell/well). The numbers of living cells after 48 hr culture are shown (green bars). Control samples before culture have been normalized to 1. n = 3; *p < 0.05.

(B–D) CD34$^-$Lin$^-$Sca-1$^+$c-kit$^+$CD150$^+$CD48$^-$ HSCs from wild-type mice were sorted and cultured in serum alone. QRT-PCR analysis of mRNA expression of HSC-specific genes (B, upper) and genes involved in cell-cycle promotion or repression (B, lower) and early myeloid differentiation (C) in HSCs before and after 6 hr culture. Results are expressed as fold difference compared to the levels found in freshly isolated HSCs from wild-type mice (G3PDH normalization). n = 3; *p < 0.05.

(D) Left: flow-cytometric analysis of RNA content of HSCs before (black line) and after (green line) 6 hr culture by PY staining. Right: flow-cytometric analysis of cell size of HSCs before (black line) and after (green line) 12 hr culture by PY staining by FSC. All error bars represent SD of the mean (A–C).

we injected these chimeric mice with 100 ng/kg DT. Flow-cytometric analysis revealed that the numbers of donor-derived CD34$^-$Lin$^-$Sca-1$^+$c-kit$^+$CD150$^+$CD48$^-$ HSCs, CLPs, pro-B cells, MEPs, proerythroblasts, and GMPs, and the cell size of donor-derived HSCs in mutant chimeras, were comparable to those observed in control chimeras 2 days after DT treatment (Figures S2B and S3B). These results indicate that a 4-fold excess of DT does not act directly on CXCL12-DTR-GFP hematopoietic cells and that the failure of hematopoiesis in DT-treated CXCL12-DTR-GFP mice was because of environmental factors.

Phenotypes of HSCs Cultured in Serum Are Similar to Those from CAR Cell-Depleted Mice

To confirm further the role of bone marrow niches for HSCs and lymphoid and erythroid progenitors, we sorted CD34$^-$Lin$^-$Sca-1$^+$c-kit$^+$CD150$^+$CD48$^-$ HSCs, CLPs, pro-B cells, and MEPs from bone marrow of wild-type mice and cultured them in serum alone. After 48 hr of single-cell cultures, many HSCs remained viable, but the numbers of living CLPs, pro-B cells, and MEPs were progressively decreased over time (Figure 4A). QRT-PCR analysis revealed that the mRNA expression of Cyclin D1, D2, A2, Cdc2a, and Cdc6 was significantly reduced, although the mRNA expression of Evi-1, Pbx1, and Mad1 was elevated in the HSC population after 6 hr of culture (Figure 4B). In addition, the mRNA expression of PU.1 and M-CSFR was markedly increased in the HSC population cultured in serum alone (Figure 4C). Flow-cytometric analysis of cultured HSCs revealed that PY fluorescence and the cell size was decreased compared with freshly isolated HSCs, although Annexin-V staining revealed no significant increase in apoptotic cells (Figure 4D and Figure S4). Together, these results demonstrate that phenotypes of wild-type HSCs and lymphoid and erythroid progenitors cultured in serum alone were similar to those from CAR cell-depleted bone marrow.

CAR Cells Are the Major Producer of SCF as Well as CXCL12 in Bone Marrow

To determine the mechanism by which CAR cells support HSCs and hematopoietic progenitors, we compared the mRNA expression of SCF and CXCL12, which are essential for the maintenance of HSCs, CLPs, and B cell and erythroid progenitors (Kohara et al., 2007; Miller et al., 1996; Sugiyama et al., 2006; Tokoyoda et al., 2004; Waskow et al., 2002), in CAR cells to other microenvironmental components of bone marrow. Flow-cytometric analysis of CXCL12-GFP mice has shown that CAR cells (CXCL12-GFP^{hi}VCAM-1$^+$CD45$^-$Ter119$^-$) constitute approximately 0.27% of nucleated cells in the bone marrow fraction. In the bone fraction, some CD45$^-$Ter119$^-$ nonhematopoietic cells have a much lower expression of CXCL12-GFP relative to CAR cells, and osteopontin (OPN)$^+$ cells have been reported to include osteoblastic niche cells (Mayack and Wagers, 2008). QRT-PCR analysis of sorted CAR cells, CD31$^+$Sca-1$^+$CD45$^-$Ter119$^-$ endothelial cells, and

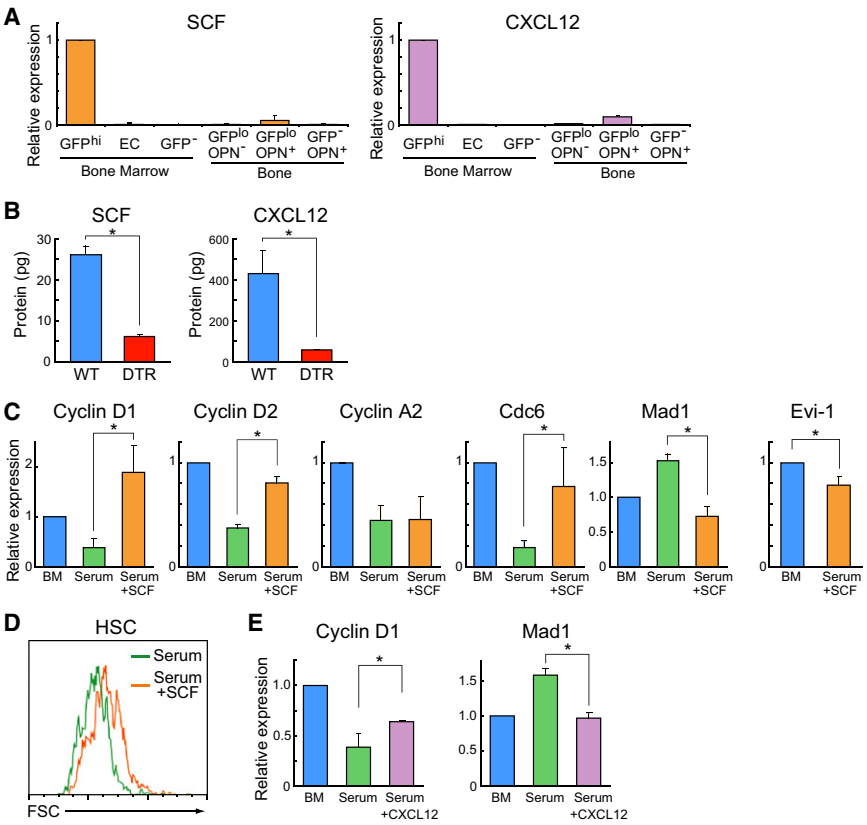

Figure 5. Preferential Expression of SCF and CXCL12 in CAR Cells

(A) QRT-PCR analysis of mRNA expression of SCF and CXCL12 in sorted CXCL12-GFP^{hi} CD45$^-$Ter119$^-$ CAR cells, CD31$^+$Sca-1$^+$CD45$^-$ Ter119$^-$ endothelial cells (ECs), and CXCL12-GFP$^-$CD31$^-$Sca-1$^-$CD45$^-$Ter119$^-$ cells from the bone marrow fraction and CXCL12-GFP^{lo}OPN$^-$, CXCL12-GFP^{lo}OPN$^+$, and CXCL12-GFP$^-$OPN$^+$ cells from the bone fraction of CXCL12-GFP mice. Results are expressed as fold difference compared to the levels found in CAR cell samples (G3PDH normalization). n = 4.

(B) The amount of SCF and CXCL12 protein per single femur from wild-type and CXCL12-DTR-GFP mice at 3 days after DT administration by enzyme-linked immunosorbent assay (ELISA). n = 3; *p < 0.05.

(C–E) CD34$^-$Lin$^-$Sca-1$^+$c-kit$^+$CD150$^+$CD48$^-$ HSCs from wild-type mice were sorted and cultured. (C) QRT-PCR analysis of mRNA expression of Cyclin D1, D2, A2, Cdc6, Mad1, and Evi-1 in HSCs before and after 6 hr culture in serum alone or with SCF. n = 3; *p < 0.05. (D) Flow-cytometric analysis of cell size of HSCs cultured in serum alone (green line) or with SCF (orange line) for 12 hr by FSC. (E) QRT-PCR analysis of mRNA expression of Cyclin D1 and Mad1 in HSCs before and after 6 hr culture in serum alone or with CXCL12. n = 3; *p < 0.05. Results are expressed as fold difference compared to the levels found in freshly isolated HSCs (G3PDH normalization) (C and E).

All error bars represent SD of the mean (A–C and E).

CXCL12-GFP$^-$CD31$^-$Sca-1$^-$CD45$^-$Ter119$^-$ cells from the bone marrow fraction, and CXCL12-GFP^{lo}OPN$^-$, CXCL12-GFP^{lo}OPN$^+$, and CXCL12-GFP$^-$OPN$^+$ cells from the bone fraction of CXCL12-GFP mice revealed that the expression of SCF and CXCL12 was considerably higher in CAR cells than in other populations examined (Figure 5A). Consistent with this, the protein expression of SCF and CXCL12 was severely reduced in the bone marrow from CAR cell-depleted mice, supporting the idea that CAR cells are the major producer of SCF and CXCL12 in the marrow (Figure 5B). Single-cell RT-PCR analysis revealed that all individual cells (52 of 52; 100%) within the CAR cell population expressed SCF in the bone marrow from CXCL12-GFP mice, suggesting that individual CAR cells express high amounts of SCF as well as CXCL12. These results are in line with the facts that SCF augments the proliferation of B cell and erythroid progenitors in culture (Martin et al., 1990), that administration of a selective inhibitor (imatinib) of c-kit, c-abl, and platelet-derived growth factor receptor (PDGFR) tyrosine kinases led to a reduction in the numbers of CLPs, pro-B cells, MEPs, and proerythroblasts and to a modest reduction in the cell size of HSCs (Figure S5), and that the numbers of CLPs, pro-B cells, and proerythroblasts are severely reduced in mice lacking SCF receptor c-kit or CAR cells.

Like HSCs from CAR cell-depleted mice, wild-type HSCs cultured in serum alone revealed altered expression of genes involved in cell-cycle promotion, DNA replication, and early myeloid differentiation and had a decreased cell size, as described above (Figures 4B–4D). SCF completely rescued the mRNA expression of Cyclin D1, D2, Cdc6, and Mad1 in HSCs (Figure 5C) and the cell size of HSCs (Figure 5D) in the culture for 6 hr. In contrast, SCF did not rescue the expression of Cyclin A2 and downregulated the expression of Evi-1 during SCF treatment (Figure 5C). In contrast, CXCL12 partially rescued the expression of Cyclin D1 and Mad1 (Figure 5E). These results suggest that SCF and CXCL12 partially contribute to the niche functions of CAR cells in HSC maintenance.

Individual CAR Cells Express both Adipogenic and Osteogenic Genes

We sought to identify the lineage nature of CAR cells. Flow-cytometric analysis of bone marrow from CXCL12-GFP mice revealed that CXCL12-GFP^{hi} CAR cells exhibited a largely homogeneous expression of cell-surface proteins, including VCAM-1, CD44, CD51 (αv integrin), PDGFRα and PDGFRβ, suggesting that CAR cells consist of a relatively homogeneous population (Figure S6A). We analyzed mRNA expression of lineage-specific markers in sorted non-hematopoietic cell populations from the bone marrow and bone fractions of CXCL12-GFP mice. QRT-PCR analysis has shown that the expressions of C/EBPα and peroxisome proliferator-activated receptor γ (PPARγ), which are essential for adipocyte differentiation (Barak et al., 1999), and Runx2 and Osterix, which are essential for osteogenic progenitors (Komori et al., 1997; Nakashima et al., 2002), were considerably higher in CAR cells than in other populations

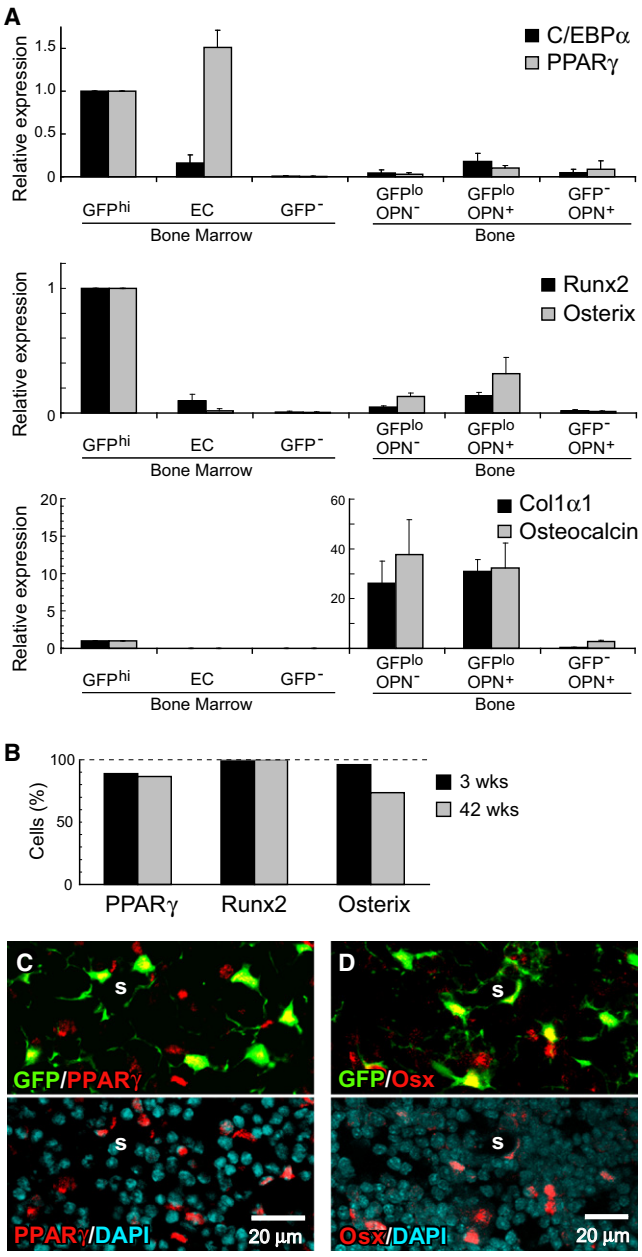

Figure 6. Expression of Requisite Factors for Adipogenesis and Osteogenesis in CAR Cells

(A) QRT-PCR analysis of sorted CXCL12-GFP^{hi}CD45^{-}Ter119^{-} CAR cells, CD31^{+}Sca-1^{+}CD45^{-}Ter119^{-} endothelial cells (ECs), and CXCL12-GFP^{-} CD31^{-}Sca-1^{-}CD45^{-}Ter119^{-} cells from the bone marrow fraction and CXCL12-GFP^{lo}OPN^{-}, CXCL12-GFP^{lo}OPN^{+}, and CXCL12-GFP^{-}OPN^{+} cells from the bone fraction of CXCL12-GFP mice. mRNA levels of C/EBPα, PPARγ, Runx2, Osterix, Col1α1, and Osteocalcin. CAR cell samples have been normalized to 1. Error bars represent SD of the mean; n = 4.

(B) Single-cell RT-PCR analysis of the frequency of cells expressing PPARγ, Runx2, and Osterix in sorted CAR cells. n = 2.

(C) Bone marrow sections from 14-week-old CXCL12-GFP mice stained with antibodies against PPARγ (red). Most CAR cells (green) express PPARγ (yellow).

(D) Bone marrow sections from 3-week-old growing CXCL12-GFP mice stained with antibodies against Osterix (red). Most CAR cells (green) express Osterix (yellow). In (C) and (D), the nuclei of cells were labeled with DAPI dye (blue); S, vascular sinus.

examined (Figure 6A). The expression of type I collagen and osteocalcin, which are abundant in osteoblasts, was much lower in CAR cells than in CXCL12-GFP^{lo}OPN^{+} or CXCL12-GFP^{lo} OPN^{-} cells from the bone fraction (Figure 6A). Furthermore, we observed a higher expression of BMPRIA and PPR, which regulate bone formation and HSC niche function (Calvi et al., 2003; Zhang et al., 2003), in CAR cells than in other cell populations (Figure S6B). To address the possibility that distinct adipogenic and osteogenic progenitors are included in the CAR cell population, we analyzed the expression of adipogenic and osteogenic genes in CAR cells at the single-cell level. Single-cell RT-PCR analysis revealed that most or all individual cells within the CAR cell population expressed PPARγ, Runx2, and Osterix in bone marrow from CXCL12-GFP mice, suggesting that most CAR cells are adipo-osteogenic bipotential progenitors (Figure 6B). Consistent with this, immunohistochemical analysis of bone marrow revealed that most CAR cells expressed PPARγ protein (Figure 6C). In addition, Osterix protein expression was observed in many CAR cells as well as bone-lining osteoblasts in 3-week-old growing CXCL12-GFP mice (Figure 6D and data not shown).

Individual CAR Cells Have Potential to Differentiate into Adipocytic and Osteoblastic Cells

We analyzed the ability of CAR cells to differentiate into adipocytic and osteoblastic cells in vitro. When CAR cells were sorted, most of these cells died immediately in culture. Thus, we cultured whole bone marrow cells from CXCL12-GFP mice in medium containing a PPARγ activator, pioglitazone. In the cultures, most CXCL12-GFP^{+} CAR cells appeared to remain viable and many CAR cells (63%) differentiated into multivacuolar lipid-containing preadipocytes, as assessed by Nile Red staining (Figures 7A and 7B), suggesting that the majority of CAR cells have the potential to differentiate into adipocytic cells in vitro. Subsequently, we cultured whole bone marrow cells from CXCL12-GFP mice in the presence of BMP-2 and analyzed the expression of an osteoblast differentiation-related marker, ALP, in individual CAR cells. In the cultures, most CAR cells appeared to remain viable, and the majority of CAR cells (90%) exhibited high ALP activity (Figure 7C and Figure S7). Because histological analysis of bone marrow has shown that only bone-lining mature osteoblasts exhibited high ALP activity (Figure 1C), these results suggest that most CAR cells have potential to differentiate into mature osteoblasts.

Next, we analyzed the ability of CAR cells to differentiate into adipocytic cells in vivo. It has been shown previously that multivacuolar lipid-containing precursors of adipocytes appear in the bone marrow of humans and mice in the early aplastic phase following chemotherapy (Bianco et al., 1988). We injected CXCL12-GFP mice with 250 mg/kg of 5-fluorouracil (5-FU), which preferentially eliminates proliferating cells. Multivacuolar lipid-containing CAR cells, as assessed by Nile Red staining, were observed in the bone marrow 7 days after 5-FU injection (Figure 7D). Some of these multivacuolar lipid-containing CAR cells surrounded sinusoidal endothelial cells, and others did

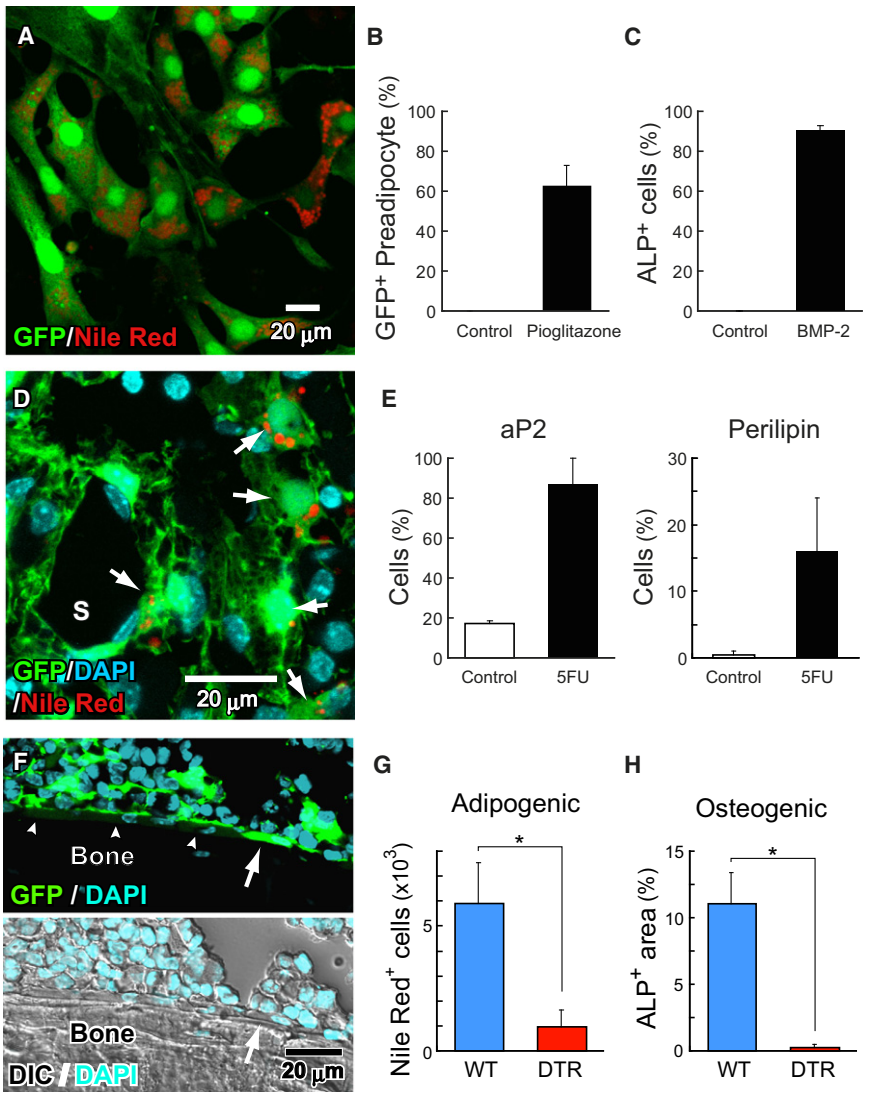

Figure 7. CAR Cells Have the Potential to Differentiate into Adipocytic and Osteoblastic Cells

(A-C) Bone marrow cells from CXCL12-GFP mice were cultured with pioglitazone (A and B) or BMP-2 (C). (A and B) After 7 days, cultures were analyzed by Nile Red staining. (A) Lipid inclusions (red) within the cytoplasm of CAR cells (green). (B) Frequency of lipid-containing cells in the whole CAR cells. (C) After 4 days, ALP activity was assayed by Fast Red staining. Frequency of ALP activity-containing cells in whole CAR cells.

(D and E) CXCL12-GFP mice were analyzed 7 days after administration of 5-FU or control vehicle. (D) Bone marrow sections stained with Nile Red. Lipid inclusions (arrows; red) within the cytoplasm of some CAR cells (green). (E) Single-cell RT-PCR analysis of the frequency of cells expressing aP2 (left) and perilipin (right) in sorted CAR cells.

(F) The bone marrow sections from 3-week-old growing CXCL12-GFP mice. Some CAR cells (green) are in contact with (arrowheads) or inserted into (arrow) the layer of mature osteoblasts lining the bone surface.

(G and H) Whole bone marrow cells from wild-type and CXCL12-DTR-GFP mice at 2 days after DT administration were cultured with pioglitazone (G) or BMP-2 (H). (G) After 7 days, cultures were analyzed by Nile Red staining. Numbers of lipid-containing cells are shown. (H) After 4 days, ALP activity was assayed by Fast Red staining. The percentage of the ALP-positive area relative to the culture area is shown. All error bars represent SD of the mean; n = 4; *p < 0.05 (B, C, E, G and H). The nuclei of cells were labeled with DAPI dye (blue) (D and F).

not (Figure 7D). Additionally, single-cell RT-PCR analysis revealed that the frequencies of cells expressing aP2, an adipocyte-specific fatty acid binding protein, and perilipin, a protein coating lipid droplets of adipocytes, which is essential for adipogenesis (Martinez-Botas et al., 2000) within CAR cells, were elevated from 17% and 0.49% in untreated mice to 87% and 16% in mice 7 days after 5-FU injection, respectively (Figure 7E), suggesting that some CAR cells differentiated into adipocytes in vivo after 5-FU-induced bone marrow hypoplasia.

In addition, immunohistochemical analysis of 3-week-old growing CXCL12-GFP mice has shown that some CAR cells are in contact with or inserted into the layer of CXCL12-GFP$^-$ mature osteoblasts lining the bone surface, raising the possibility that CAR cells near the bone surface differentiate into mature osteoblasts in vivo (Figure 7F). Together, these results suggest that the majority of CAR cells have the potential to differentiate into adipocytic and osteoblastic cells, and the differentiation of some CAR cells occurs in vivo.

Finally, we analyzed the ability of CAR cell-depleted bone marrow cells to differentiate into adipocytic and osteoblastic cells. We cultured whole bone marrow cells from DT-treated CXCL12-DTR-GFP mice and control animals in medium containing pioglitazone or BMP-2. The numbers of lipid-containing adipocytic cells or marked ALP activity-containing osteoblastic cells were severely reduced in cultures from CAR cell-depleted bone marrow cells compared with cultures from control bone marrow cells, as assessed by Nile Red or Fast Red staining, respectively (Figures 7G and 7H and data not shown). These results support the idea that CAR cells are progenitors of adipocytes and osteoblasts within bone marrow.

DISCUSSION

In this study, we determined the in vivo essential role of CAR cells as the niche for HSCs and lymphoid and erythroid progenitors, using DT-treated CXCL12-DTR-GFP mice in which CAR cells were selectively lost but other candidate niches, including bone-lining osteoblasts, SNO cells, and endothelial cells, were still present. Together with the significant mRNA expression of Col1α1 in CAR cells, there is a possibility that CAR cells were decreased in the Col2.3ΔTK mice depleted of cells with the rat Col1α1 gene promoter driving thymidine kinase, in which B cells and erythrocytes were reduced (Visnjic et al., 2004). In addition,

because CAR cells exhibited high expression of BMPRIA and PPR, which have been reported to control HSC numbers, BMPRIA and/or PPR might regulate niche functions of CAR cells.

HSCs remained viable much longer than lymphoid and erythroid progenitors during cultures in serum alone and display similar phenotypes to HSCs from CAR cell-depleted mice. Considering that serum contains widely diffusible signals present in the circulation and marrow non-niche microenvironment, these results suggest that CAR cells are the major producer of specific niche signals for HSCs and hematopoietic progenitors in bone marrow. Because our results indicate that CAR cells are the major producer of SCF and CXCL12, which are essential for the maintenance of HSCs and lymphoid and erythroid progenitors, SCF and CXCL12 would contribute in concert with other factors to the niche functions of CAR cells.

Recent studies using label-retaining assays have identified a highly dormant small subpopulation (~30%) of HSCs, termed dormant HSCs (d-HSCs), dividing about every 145 days, and another rarely dividing activated HSC (a-HSCs) subpopulation (~70%) dividing around every 36 days, within the $CD34^{-}Lin^{-}Sca\text{-}1^{+}c\text{-}kit^{+}CD150^{+}CD48^{-}$ HSC population of bone marrow (Wilson et al., 2008). Considering that HSCs were reduced and more quiescent in the absence of CAR cells, this raises the possibility that a-HSCs were selectively lost or returned to a d-HSC status in CAR cell-depleted mice. Further studies will be needed to determine the role of CAR cells in the maintenance of d-HSCs and a-HSCs.

Our findings suggest that CAR cells maintain both HSCs and B cell and erythroid progenitors in a proliferative state; however, HSCs are cycling slowly, although B cell and erythroid progenitors are cycling much more rapidly. How can we explain the difference? Infrequent division of HSCs may be controlled by HSC-intrinsic mechanisms. An alternative explanation is that CAR cells or other microenvironmental components located near CAR cells, including endothelial cells, provide signals that slow the proliferation of HSCs, but not lymphoid or erythroid progenitors. Candidates include Angiopoietin-1, Wnts, and TGF-βs, which have been reported to slow the proliferation of HSCs (Arai et al., 2004; Fleming et al., 2008; Yamazaki et al., 2009). In contrast, critical lineage-specific soluble factors, including IL-7 and erythropoietin, augment the proliferation of lymphoid and erythroid progenitors, respectively, but not HSCs.

Although niche signals maintain stem cells in an undifferentiated state in *Drosophila* gonads (Xie and Spradling, 1998), it remains unclear whether vertebrate HSC niches employ an analogous mechanism. Our findings that HSCs from CAR cell-depleted mice have a markedly increased mRNA expression of PU.1 and generate substantial numbers of myeloid lineage cells in culture earlier than the wild-type suggest that CAR cells keep HSCs in an undifferentiated state. It may be that myeloid differentiation of HSCs is a default pathway in the absence of niche signals that maintain HSCs in a proliferative state. Alternatively, CAR cells may provide signals which inhibit the myeloid differentiation of HSCs controlled by non-CAR cell microenvironmental factors and/or HSC-intrinsic mechanisms.

At 2 days after the induction of CAR cell ablation, the numbers of HSCs were reduced about 50% in the marrow. Because it has been reported that only about 4% of HSCs are proliferating at any given time (Kiel et al., 2005) and that HSCs divide every 36 or 145 days (Wilson et al., 2008), HSC reduction over 2 days in CAR cell-depleted mice cannot be explained simply by the results that CAR cells maintain HSCs in a proliferative state. It is likely that enhanced differentiation of some HSCs caused HSC reduction in CAR cell-depleted mice. In addition, although no increase in Annexin-V-positive apoptotic cells in the HSC fraction and the accumulation of HSCs in the circulation was observed in CAR cell-depleted mice, there is a possibility that CAR cells are also involved in supporting the survival and/or retention of HSCs within bone marrow.

CXCL12-DTR-GFP mice died probably from liver failure 5 days after DT treatment and it should also be noted that thrombopoietin (TPO), which plays a critical role in hematopoiesis is predominantly expressed in liver (Lok et al., 1994). However, at 2 days after DT treatment, the liver of CXCL12-DTR-GFP mice in which bone marrow hematopoiesis was affected appeared normal macroscopically and histologically, and had normal expression of TPO mRNA by qRT-PCR analysis (data not shown). In addition, there was no reduction of TPO protein in peripheral blood of the DT-treated CXCL12-DTR-GFP mice (data not shown). These results suggest that the liver of CXCL12-DTR-GFP mice did not cause the hematopoietic abnormalities 2 days after DT treatment. On the other hand, in the bone marrow of DT-treated CXCL12-DTR-GFP mice in which the numbers of CAR cells were reduced, the size of HSCs in contact with the remaining CAR cells was normal, although the size of HSCs which did not adjoin CAR cells was significantly reduced by histological analysis. Together, it is likely that phenotypes observed in the marrow of CXCL12-DTR-GFP mice were because of loss of CAR cells 2 days after DT treatment.

Our results do not rule out the possibility that other candidate niches, including SNO cells and endothelial cells, play an important role in hematopoiesis. The results that the numbers of MPPs, $CCR9^{+}$MPPs, and $CD122^{+}NK1.1^{-}$ NK progenitors were normal, although CLPs and $CCR9^{+}$CLPs (Zlotoff et al., 2010) were reduced in DT-treated CXCL12-DTR-GFP mice (Figure S2C), suggest that progenitors for distinct lymphoid lineages may inhabit different niches and have different requirements in bone marrow. Because many CAR cells are perivascular, interaction between CAR cells and endothelial cells may be important in the construction of HSC niches. Experiments using mice that allow the selective depletion of SNO cells or sinusoidal endothelial cells will be needed to determine the niche functions of these cells.

We have suggested that CAR cells are adipo-osteogenic progenitors, which produce large amounts of hematopoietic cytokines, CXCL12 and SCF, before they differentiate into mature cells producing large amounts of proteins for the storage of nutritional energy or bone formation. Previous studies have shown that adventitial reticular cells covering the endothelium of vascular sinuses give rise to adipocytes (Bianco et al., 1988) and that osteogenic progenitors are present in the intertrabecular space of bone marrow (Rouleau et al., 1990). Our results explain this discrepancy and suggest an essential in vivo role of adipo-osteogenic progenitors in bone marrow. In addition, our findings raise the possibility that differentiation of CAR cells into adipocytic and/or osteoblastic cells alters their niche functions. Together, our findings provide a basis for understanding

how microenvironmental niches regulate HSC maintenance and lympho-hematopoiesis within bone marrow.

EXPERIMENTAL PROCEDURES

Mice

CXCL12-GFP mice (Ara et al., 2003) and CXCL12-DTR-GFP mice were maintained on a C57BL/6 background. 5-FU (Kyowa Hakko Kirin) was injected intraperitoneally into 12- to 15-week-old mice. Imatinib (Glivec; Novartis) was applied by oral gavage (twice a day, 200 mg/kg/day). All experiments were performed under guidelines of the animal ethics committee of Institute for Frontier Medical Sciences, Kyoto University.

Generation of CXCL12-DTR-GFP Mice

The targeting vector was generated as shown in Figure 1A. The neo cassette was removed from the recombinant allele by Cre-recombinase in vivo. CXCL12-DTR-GFP mice were backcrossed to C57BL/6 mice six times. DT (MBL) was injected intraperitoneally into 12- to 15-week-old mice.

Antibodies

The antibodies used were described in Supplemental Experimental Procedures.

Flow-Cytometric Analysis and Cell Sorting

Cell-cycle analysis was performed as described in our previous publication (Sugiyama et al., 2006). For the apoptosis assay, Annexin V-FITC Apoptosis Detection Kit I (BD Biosystems) was used according to the manufacturer's instruction. All flow-cytometric experiments and cell sorting were performed using a BD FACSAria (BD Biosystems). For sorting the nonhematopoietic cell populations, cells in bone marrow fraction were obtained from femurs and tibiae by flushing and collagenase (Sigma) digestion, and cells in bone fraction were obtained from marrow-depleted bones by mechanical disruption and collagenase digestion (Mayack and Wagers, 2008).

Competitive Repopulation Assay

Unfractionated 1/20 of bone marrow cells from two femurs and tibiae (C57BL/6-Ly5.2$^+$ background) to be tested were mixed with 1 × 10^6 bone marrow cells of C57BL/6-Ly5.1$^+$ mice as competitor cells and were transplanted into lethally irradiated (9 Gy) C57BL/6-Ly5.1$^+$ mice. Peripheral blood cells of the recipient mice were taken 12 weeks after transplantation, and myeloid cells were analyzed by flow cytometer because their high turnover provides a good measure of HSC activity. Repopulating Units (RU) were calculated using Harrison's formula as described previously (Harrison et al., 1993).

Cell Culture and Analysis

For stromal cell-free culture, cells were sorted from wild-type mice and cultured in RPMI-1640 medium (Invitrogen) or S clone SF-3 medium (Sanko Junyaku) containing 10% fetal calf serum (FCS) with or without 20 ng/ml SCF (R&D Systems) or 1 μg/ml CXCL12. Cultured PI$^-$ viable cells were resorted and analyzed.

For adipogenic differentiation, bone marrow cell suspensions were cultured on a collagen-coated dish in DMEM supplemented with pioglitazone (Takeda Pharmaceutical) (10 μM), 10% FCS, and 5 × 10^{-5} M 2-β-mercaptoethanol for 7 days. To visualize lipid droplets, PFA fixation and Nile Red staining were performed. For osteogenic differentiation, bone marrow cell suspensions were cultured in α-MEM supplemented with BMP-2 (R&D Systems) (300 ng/ml), 10% FCS, and 5 × 10^{-5} M 2-β-mercaptoethanol for 4 days. Osteoblastic phenotypes were evaluated by the activity of ALP using Fast Red staining.

Immunohistochemical Analysis

Bone marrow sections were analyzed by immunofluorescence as described previously (Sugiyama et al., 2006). To visualize lipid droplets, Nile Red staining was performed. Confocal microscopy was performed with a LSM 510 META (Carl Zeiss).

QRT-PCR Analysis

Total RNA was isolated from sorted cells using Isogen (Nippon Gene) and treated with DNase I (Invitrogen). cDNA was synthesized using SuperScript VILO (Invitrogen) following the manufacturer's instructions. QRT-PCR analysis was performed with a Step One Plus (Applied Biosystems) using Power SYBR Green PCR Master Mix (Applied Biosystems). Values for each gene were normalized to the relative quantity of *Gapdh* mRNA in each sample. The primers used for PCR are listed in Supplemental Experimental Procedures.

Single-Cell RT-PCR Analysis

Single cells were sorted into reverse transcription buffer containing 1 U/μl RNase Inhibitor (Toyobo) and 0.4% Nonidet P-40 (Nacalai Tesque) using flow cytometry. Cell lysates were reverse-transcribed using M-MLV reverse transcriptase (Toyobo) and gene-specific reverse primers. PCR was performed by the addition of premixed hot-start PCR enzymes and buffers (AmpliTaq Gold; Applied Biosystems) containing the gene-specific forward and reverse primers designed to span introns to exclude genomic products. PCR was carried out in one round with 50 amplification cycles. The primers used for PCR are listed in Supplemental Experimental Procedures.

ELISA

Femurs were flushed with 0.3 ml of PBS containing a protease inhibitor cocktail (Sigma) and Nonidet P40 (1%). Cells were lysed by freeze and thaw, and the cell debris was removed by centrifugation and discarded. The concentrations of SCF and CXCL12 were measured using DuoSet ELISA Development kits (R&D Systems) according to the manufacturer's instructions.

Statistical Analysis

The significance of the difference between groups in the experiments was evaluated by analysis of variance followed by a two-tailed Student's t test.

SUPPLEMENTAL INFORMATION

Supplemental Information includes seven figures and Supplemental Experimental Procedures and can be found with this article online at doi:10.1016/j.immuni.2010.08.017.

ACKNOWLEDGMENTS

We thank T. Egawa, K. Tokoyoda, M. Noda, R. Kamimura, T. Ishii, and S. Uemoto for technical assistance. This work was supported by grants from the Ministry of Education, Science, Sports and Culture of Japan. Y. O., T. S., and T. N. designed and performed the experiments, analyzed the data, and prepared the paper; T. N. supervised the study; H.K. performed the experiments; G. K., N.F., and K. K. contributed materials and tools.

Received: February 3, 2010
Revised: June 12, 2010
Accepted: August 13, 2010
Published online: September 16, 2010

REFERENCES

Adolfsson, J., Borge, O.J., Bryder, D., Theilgaard-Mönch, K., Astrand-Grundström, I., Sitnicka, E., Sasaki, Y., and Jacobsen, S.E. (2001). Upregulation of Flt3 expression within the bone marrow Lin(-)Sca1(+)c-kit(+) stem cell compartment is accompanied by loss of self-renewal capacity. Immunity *15*, 659–669.

Akashi, K., Traver, D., Miyamoto, T., and Weissman, I.L. (2000). A clonogenic common myeloid progenitor that gives rise to all myeloid lineages. Nature *404*, 193–197.

Ara, T., Tokoyoda, K., Sugiyama, T., Egawa, T., Kawabata, K., and Nagasawa, T. (2003). Long-term hematopoietic stem cells require stromal cell-derived factor-1 for colonizing bone marrow during ontogeny. Immunity *19*, 257–267.

Arai, F., Hirao, A., Ohmura, M., Sato, H., Matsuoka, S., Takubo, K., Ito, K., Koh, G.Y., and Suda, T. (2004). Tie2/angiopoietin-1 signaling regulates hematopoietic stem cell quiescence in the bone marrow niche. Cell *118*, 149–161.

Arinobu, Y., Mizuno, S., Chong, Y., Shigematsu, H., Iino, T., Iwasaki, H., Graf, T., Mayfield, R., Chan, S., Kastner, P., and Akashi, K. (2007). Reciprocal activation of GATA-1 and PU.1 marks initial specification of hematopoietic stem

cells into myeloerythroid and myelolymphoid lineages. Cell Stem Cell *1*, 416–427.

Barak, Y., Nelson, M.C., Ong, E.S., Jones, Y.Z., Ruiz-Lozano, P., Chien, K.R., Koder, A., and Evans, R.M. (1999). PPAR gamma is required for placental, cardiac, and adipose tissue development. Mol. Cell *4*, 585–595.

Bianco, P., Costantini, M., Dearden, L.C., and Bonucci, E. (1988). Alkaline phosphatase positive precursors of adipocytes in the human bone marrow. Br. J. Haematol. *68*, 401–403.

Calvi, L.M., Adams, G.B., Weibrecht, K.W., Weber, J.M., Olson, D.P., Knight, M.C., Martin, R.P., Schipani, E., Divieti, P., Bringhurst, F.R., et al. (2003). Osteoblastic cells regulate the haematopoietic stem cell niche. Nature *425*, 841–846.

Cheshier, S.H., Morrison, S.J., Liao, X., and Weissman, I.L. (1999). In vivo proliferation and cell cycle kinetics of long-term self-renewing hematopoietic stem cells. Proc. Natl. Acad. Sci. USA *96*, 3120–3125.

DeKoter, R.P., and Singh, H. (2000). Regulation of B lymphocyte and macrophage development by graded expression of PU.1. Science *288*, 1439–1441.

Ficara, F., Murphy, M.J., Lin, M., and Cleary, M.L. (2008). Pbx1 regulates self-renewal of long-term hematopoietic stem cells by maintaining their quiescence. Cell Stem Cell *2*, 484–496.

Fleming, H.E., Janzen, V., Lo Celso, C., Guo, J., Leahy, K.M., Kronenberg, H.M., and Scadden, D.T. (2008). Wnt signaling in the niche enforces hematopoietic stem cell quiescence and is necessary to preserve self-renewal in vivo. Cell Stem Cell *2*, 274–283.

Foudi, A., Hochedlinger, K., Van Buren, D., Schindler, J.W., Jaenisch, R., Carey, V., and Hock, H. (2009). Analysis of histone 2B-GFP retention reveals slowly cycling hematopoietic stem cells. Nat. Biotechnol. *27*, 84–90.

Goyama, S., Yamamoto, G., Shimabe, M., Sato, T., Ichikawa, M., Ogawa, S., Chiba, S., and Kurokawa, M. (2008). Evi-1 is a critical regulator for hematopoietic stem cells and transformed leukemic cells. Cell Stem Cell *3*, 207–220.

Harrison, D.E., Jordan, C.T., Zhong, R.K., and Astle, C.M. (1993). Primitive hemopoietic stem cells: direct assay of most productive populations by competitive repopulation with simple binomial, correlation and covariance calculations. Exp. Hematol. *21*, 206–219.

Iritani, B.M., Delrow, J., Grandori, C., Gomez, I., Klacking, M., Carlos, L.S., and Eisenman, R.N. (2002). Modulation of T-lymphocyte development, growth and cell size by the Myc antagonist and transcriptional repressor Mad1. EMBO J. *21*, 4820–4830.

Kalaszczynska, I., Geng, Y., Iino, T., Mizuno, S., Choi, Y., Kondratiuk, I., Silver, D.P., Wolgemuth, D.J., Akashi, K., and Sicinski, P. (2009). Cyclin A is redundant in fibroblasts but essential in hematopoietic and embryonic stem cells. Cell *138*, 352–365.

Karsunky, H., Inlay, M.A., Serwold, T., Bhattacharya, D., and Weissman, I.L. (2008). Flk2+ common lymphoid progenitors possess equivalent differentiation potential for the B and T lineages. Blood *111*, 5562–5570.

Kiel, M.J., Yilmaz, O.H., Iwashita, T., Yilmaz, O.H., Terhorst, C., and Morrison, S.J. (2005). SLAM family receptors distinguish hematopoietic stem and progenitor cells and reveal endothelial niches for stem cells. Cell *121*, 1109–1121.

Kiel, M.J., Radice, G.L., and Morrison, S.J. (2007). Lack of evidence that hematopoietic stem cells depend on N-cadherin-mediated adhesion to osteoblasts for their maintenance. Cell Stem Cell *1*, 204–217.

Kohara, H., Omatsu, Y., Sugiyama, T., Noda, M., Fujii, N., and Nagasawa, T. (2007). Development of plasmacytoid dendritic cells in bone marrow stromal cell niches requires CXCL12-CXCR4 chemokine signaling. Blood *110*, 4153–4160.

Komori, T., Yagi, H., Nomura, S., Yamaguchi, A., Sasaki, K., Deguchi, K., Shimizu, Y., Bronson, R.T., Gao, Y.H., Inada, M., et al. (1997). Targeted disruption of Cbfa1 results in a complete lack of bone formation owing to maturational arrest of osteoblasts. Cell *89*, 755–764.

Kozar, K., Ciemerych, M.A., Rebel, V.I., Shigematsu, H., Zagozdzon, A., Sicinska, E., Geng, Y., Yu, Q., Bhattacharya, S., Bronson, R.T., et al. (2004). Mouse development and cell proliferation in the absence of D-cyclins. Cell *118*, 477–491.

Lok, S., Kaushansky, K., Holly, R.D., Kuijper, J.L., Lofton-Day, C.E., Oort, P.J., Grant, F.J., Heipel, M.D., Burkhead, S.K., Kramer, J.M., et al. (1994). Cloning and expression of murine thrombopoietin cDNA and stimulation of platelet production in vivo. Nature *369*, 565–568.

Martin, F.H., Suggs, S.V., Langley, K.E., Lu, H.S., Ting, J., Okino, K.H., Morris, C.F., McNiece, I.K., Jacobsen, F.W., Mendiaz, E.A., et al. (1990). Primary structure and functional expression of rat and human stem cell factor DNAs. Cell *63*, 203–211.

Martinez-Botas, J., Anderson, J.B., Tessier, D., Lapillonne, A., Chang, B.H., Quast, M.J., Gorenstein, D., Chen, K.H., and Chan, L. (2000). Absence of perilipin results in leanness and reverses obesity in Lepr(db/db) mice. Nat. Genet. *26*, 474–479.

Mayack, S.R., and Wagers, A.J. (2008). Osteolineage niche cells initiate hematopoietic stem cell mobilization. Blood *112*, 519–531.

Miller, C.L., Rebel, V.I., Lemieux, M.E., Helgason, C.D., Lansdorp, P.M., and Eaves, C.J. (1996). Studies of W mutant mice provide evidence for alternate mechanisms capable of activating hematopoietic stem cells. Exp. Hematol. *24*, 185–194.

Morrison, S.J., and Spradling, A.C. (2008). Stem cells and niches: mechanisms that promote stem cell maintenance throughout life. Cell *132*, 598–611.

Nagasawa, T. (2006). Microenvironmental niches in the bone marrow required for B-cell development. Nat. Rev. Immunol. *6*, 107–116.

Nagasawa, T. (2008). New niches for B cells. Nat. Immunol. *9*, 345–346.

Nagasawa, T., Kikutani, H., and Kishimoto, T. (1994). Molecular cloning and structure of a pre-B-cell growth-stimulating factor. Proc. Natl. Acad. Sci. USA *91*, 2305–2309.

Nagasawa, T., Hirota, S., Tachibana, K., Takakura, N., Nishikawa, S., Kitamura, Y., Yoshida, N., Kikutani, H., and Kishimoto, T. (1996). Defects of B-cell lymphopoiesis and bone-marrow myelopoiesis in mice lacking the CXC chemokine PBSF/SDF-1. Nature *382*, 635–638.

Nakashima, K., Zhou, X., Kunkel, G., Zhang, Z., Deng, J.M., Behringer, R.R., and de Crombrugghe, B. (2002). The novel zinc finger-containing transcription factor osterix is required for osteoblast differentiation and bone formation. Cell *108*, 17–29.

Orford, K.W., and Scadden, D.T. (2008). Deconstructing stem cell self-renewal: genetic insights into cell-cycle regulation. Nat. Rev. Genet. *9*, 115–128.

Rouleau, M.F., Mitchell, J., and Goltzman, D. (1990). Characterization of the major parathyroid hormone target cell in the endosteal metaphysis of rat long bones. J. Bone Miner. Res. *5*, 1043–1053.

Saito, M., Iwawaki, T., Taya, C., Yonekawa, H., Noda, M., Inui, Y., Mekada, E., Kimata, Y., Tsuru, A., and Kohno, K. (2001). Diphtheria toxin receptor-mediated conditional and targeted cell ablation in transgenic mice. Nat. Biotechnol. *19*, 746–750.

Santaguida, M., Schepers, K., King, B., Sabnis, A.J., Forsberg, E.C., Attema, J.L., Braun, B.S., and Passegué, E. (2009). JunB protects against myeloid malignancies by limiting hematopoietic stem cell proliferation and differentiation without affecting self-renewal. Cancer Cell *15*, 341–352.

Sugiyama, T., Kohara, H., Noda, M., and Nagasawa, T. (2006). Maintenance of the hematopoietic stem cell pool by CXCL12-CXCR4 chemokine signaling in bone marrow stromal cell niches. Immunity *25*, 977–988.

Tachibana, K., Hirota, S., Iizasa, H., Yoshida, H., Kawabata, K., Kataoka, Y., Kitamura, Y., Matsushima, K., Yoshida, N., Nishikawa, S., et al. (1998). The chemokine receptor CXCR4 is essential for vascularization of the gastrointestinal tract. Nature *393*, 591–594.

Tokoyoda, K., Egawa, T., Sugiyama, T., Choi, B.I., and Nagasawa, T. (2004). Cellular niches controlling B lymphocyte behavior within bone marrow during development. Immunity *20*, 707–718.

Visnjic, D., Kalajzic, Z., Rowe, D.W., Katavic, V., Lorenzo, J., and Aguila, H.L. (2004). Hematopoiesis is severely altered in mice with an induced osteoblast deficiency. Blood *103*, 3258–3264.

Walkley, C.R., Fero, M.L., Chien, W.M., Purton, L.E., and McArthur, G.A. (2005). Negative cell-cycle regulators cooperatively control self-renewal and differentiation of haematopoietic stem cells. Nat. Cell Biol. *7*, 172–178.

Waskow, C., Paul, S., Haller, C., Gassmann, M., and Rodewald, H.R. (2002). Viable c-Kit(W/W) mutants reveal pivotal role for c-kit in the maintenance of lymphopoiesis. Immunity *17*, 277–288.

Wilson, A., and Trumpp, A. (2006). Bone-marrow haematopoietic-stem-cell niches. Nat. Rev. Immunol. *6*, 93–106.

Wilson, A., Laurenti, E., Oser, G., van der Wath, R.C., Blanco-Bose, W., Jaworski, M., Offner, S., Dunant, C.F., Eshkind, L., Bockamp, E., et al. (2008). Hematopoietic stem cells reversibly switch from dormancy to self-renewal during homeostasis and repair. Cell *135*, 1118–1129.

Xie, T., and Spradling, A.C. (1998). decapentaplegic is essential for the maintenance and division of germline stem cells in the *Drosophila* ovary. Cell *94*, 251–260.

Yamazaki, S., Iwama, A., Takayanagi, S., Morita, Y., Eto, K., Ema, H., and Nakauchi, H. (2006). Cytokine signals modulated via lipid rafts mimic niche signals and induce hibernation in hematopoietic stem cells. EMBO J. *25*, 3515–3523.

Yamazaki, S., Iwama, A., Takayanagi, S., Eto, K., Ema, H., and Nakauchi, H. (2009). TGF-beta as a candidate bone marrow niche signal to induce hematopoietic stem cell hibernation. Blood *113*, 1250–1256.

Zhang, J., Niu, C., Ye, L., Huang, H., He, X., Tong, W.G., Ross, J., Haug, J., Johnson, T., Feng, J.Q., et al. (2003). Identification of the haematopoietic stem cell niche and control of the niche size. Nature *425*, 836–841.

Zhu, J., Garrett, R., Jung, Y., Zhang, Y., Kim, N., Wang, J., Joe, G.J., Hexner, E., Choi, Y., Taichman, R.S., and Emerson, S.G. (2007). Osteoblasts support B-lymphocyte commitment and differentiation from hematopoietic stem cells. Blood *109*, 3706–3712.

Zlotoff, D.A., Sambandam, A., Logan, T.D., Bell, J.J., Schwarz, B.A., and Bhandoola, A. (2010). CCR7 and CCR9 together recruit hematopoietic progenitors to the adult thymus. Blood *115*, 1897–1905.

Zou, Y.R., Kottmann, A.H., Kuroda, M., Taniuchi, I., and Littman, D.R. (1998). Function of the chemokine receptor CXCR4 in haematopoiesis and in cerebellar development. Nature *393*, 595–599.